

The Use of Boundary Elements For The Determination of The AGMA Geometry Factor

Sandeep M. Vijayakar
Donald R. Houser
The Ohio State University
Columbus, Ohio

Abstract:

The traditional method of computing the geometry factor has limitations in its consideration of internal gears, gears with thin rims or gears with rims having complexities such as spokes and holes. The finite element method may be used in such instances, but is often time consuming for both model development and computation. The boundary element method described in this article, provides an alternative which is easier to set up and allows one to compute geometry factors for many tooth configurations. The examples shown in this article use the boundary element method to show how the peak stress amplitude and its location change with different rim thickness and support conditions.

Introduction

The geometry factor, which is a fundamental part of the AGMA strength rating of gears, is currently computed using the Lewis parabola which allows computation of the Lewis form factor.⁽¹⁾ The geometry factor is obtained from this Lewis factor by applying a stress correction factor, a helical overlap factor and load sharing ratio. This method, which originally required graphical construction methods and more recently has been computerized, works reasonably well for external gears with thick rims.⁽²⁻⁶⁾ However, when thin rims are encountered or when evaluating the strength of internal gears, the AGMA method cannot be used. When these situations are encountered, most investigators have used finite elements to determine the maximum tooth root stresses. Examples of such analyses for thin rimmed gears are presented by Drago,^(7,8) Suzuki et al,⁽⁹⁾ Chong and Kubo⁽¹⁰⁾ and Eloranta.⁽¹¹⁾ Castellani and Castelli⁽¹²⁾ compare both AGMA and ISO rating methods with finite element results. In addition, Chong et al^(13,14) have developed an approximate formula for the analysis of thin rimmed gears. Ishida et al^(15,16) and Drago⁽¹⁷⁾ present measured stress data for thin rimmed gears. The state of stress for internal gears has been analyzed by numerous investigators.⁽¹⁸⁻²⁴⁾

The previous investigators have shown that the assumptions of the AGMA method for thin rimmed gears and for internal gears cannot be used successfully. The finite element method is viable, but because of time consuming procedures

in creating a model and in handling unusual boundary shapes, it can be quite burdensome and will usually require considerable computer power, even for two dimensional elements. An analysis procedure which shows promise, both from a model building standpoint and from computational efficiency, is the boundary element method.^(25,26) This method, which has some of the features of the finite element method, has been applied to gears by Gakwaya et al.⁽²⁷⁾ Rubenchik⁽²⁸⁾ used a similar method called the boundary integral method for the computation of root stresses. The paper by Oda et al,⁽³¹⁾ etc. which appeared at the same time that this article was being prepared, carries out an extensive comparison between the stresses at the roots of thin rimmed external and internal gears by the boundary element method, the finite element method and from experiments. Since the boundary element method potentially can be used on personal computers and models can be easily developed, this article presents an introductory study of its potential in computing geometry factors.

Subsequent sections of this article outline the fundamental theory of the boundary element method and present some preliminary results. The computational procedure is such that

AUTHORS:

DR. SANDEEP M. VIJAYAKAR received his B'Tech degree from the Indian Institute of Technology at Bombay and his M.S. and Ph.D. from Ohio State University. He is currently a research associate at Ohio State and a member of ASME.

DR. DONALD R. HOUSER is on the faculty of the Department of Mechanical Engineering, Ohio State University. In addition to his teaching responsibilities, he has researched and published in the areas of gear dynamics and noise, v-belts, vibration diagnostics and vibration signal analysis. He is also currently director of the university's Gear Dynamics and Gear Noise Research Laboratory. Dr. Houser is a member of ASME, SAE, AGMA and Tau Beta Pi, Pi Tau Sigma and Sigma Xi honorary fraternities. He is also chairman of the ASME Power Transmission and Gearing Committee. Dr. Houser received his degrees in mechanical engineering from the University of Wisconsin at Madison.

(continued from page 9)

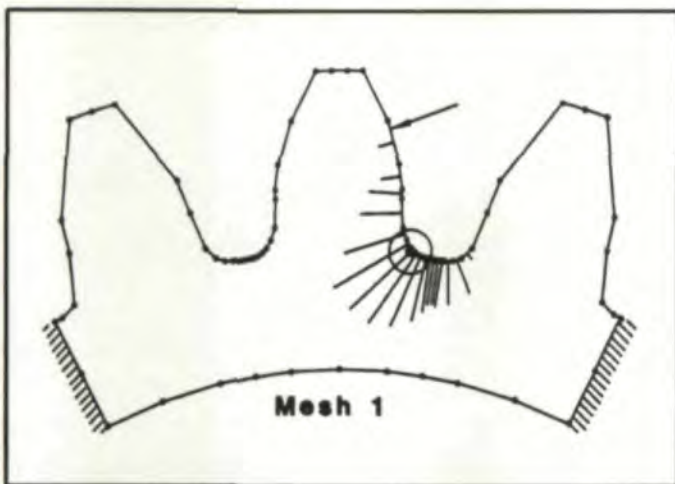


Fig. 3—Stress distribution along the boundary for a thick rimmed external gear supported at the ends.

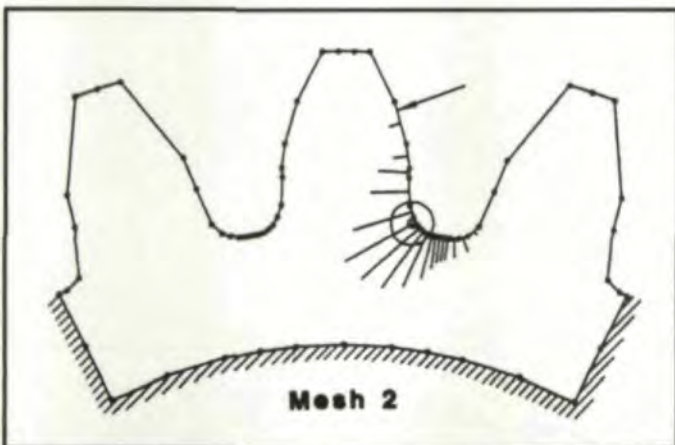


Fig. 4—Stress distribution along the boundary for a thick rimmed external gear supported along the inner bore.

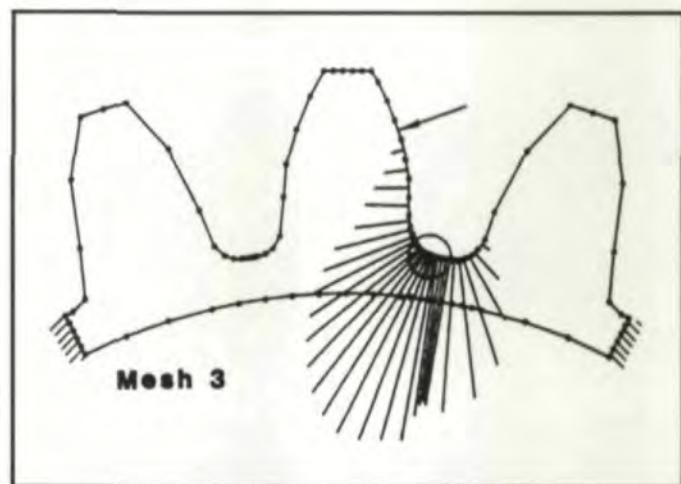


Fig. 5—Stress distribution along the boundary for a thin rimmed external gear supported at the ends.

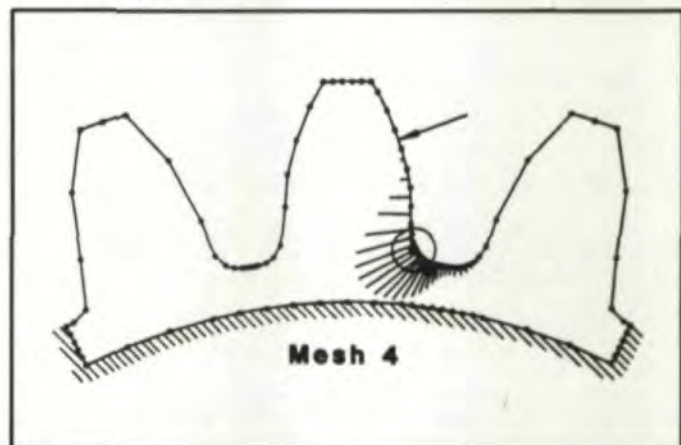


Fig. 6—Stress distribution along the boundary for a thin rimmed external gear supported along the inner bore.

of the critical stress point did not change, and the J factor was found to increase from 0.335 to 0.343 just by changing the boundary conditions. Mesh 3 (Fig. 5) shows a thin rimmed gear whose rim is unsupported, and Mesh 4 (Fig. 6) shows the same thin rimmed gear with a fixed rim. The boundary condition effect on the J factor is much greater for the thin rimmed case, and the stresses increase when the constraints for the thin rimmed case are removed. The location of the critical point also changes. A computer analysis using the AGMA 218.01 standard gave a value of 0.3019 for the J factor for cases 1 through 4, and the graphs in the AGMA standard give a J factor of about 0.32. Finite element models were also created and run on ANSYS for cases 1 through 4. Fig. 10 shows the finite element model for case 4, and Fig. 11 shows the contour plot of the maximum principal stress for this run. The J factors from the finite element runs are also tabulated in Table 1. The finite element models show stresses that are consistently 10% higher than those obtained by the boundary element models. This may be due to the different techniques used by the two methods in extrapolating the stresses to the surface and needs further investigation. Table 3 shows J factors obtained for gear teeth with the same profile and roots as in cases 1 through 4, as the inner radius is

varied from 0.5 to 0.8, with the rim supported only at its edges.

Meshes 5 and 6 (Figs. 7 & 8) show that this approach can also be used with internal gears, and Mesh 7 (Fig. 9) shows how this method can be used with gears with a small number of teeth when undercutting takes place. Plane stress conditions were assumed for these cases, but plane strain conditions could have been used. The decision as to which is more applicable would have to be made by the user.

Summary and Future Research

The boundary element methodology has several advantages over using the standardized gear rating schemes. It can take into account different boundary conditions, account for plane stress or plane strain conditions, determine the actual critical point and include the effects of support conditions and rim thickness. Furthermore, the method can handle internal gears and can also compute displacements. Since the complete multi-axial state of stress at any point is available, any failure theory can be used to identify the critical point and to compute the geometry factor.

The method does, however, have limitations. The state of stress in gear teeth is almost always three-dimensional, and

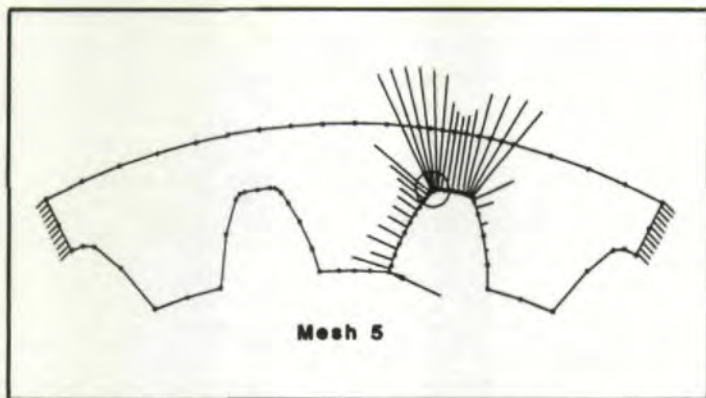


Fig. 7—Stress distribution along the boundary for an internal gear supported at the ends.

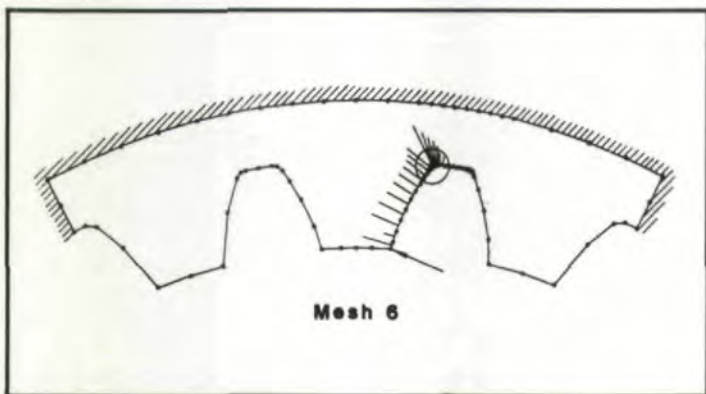


Fig. 8—Stress distribution along the boundary for an internal gear supported along the outer radius.

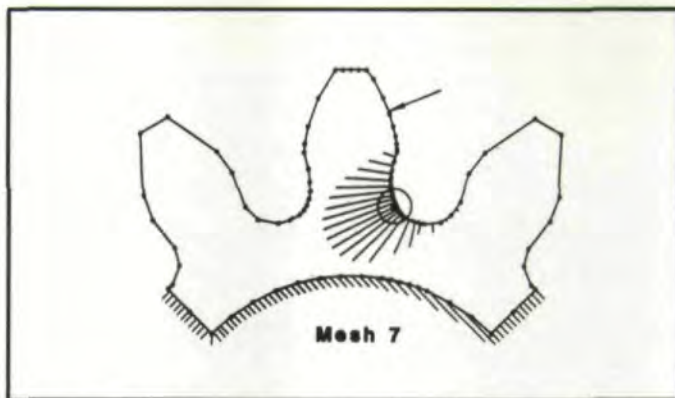


Fig. 9—Stress distribution along the boundary for an external gear with 12 teeth supported along the inner bore.

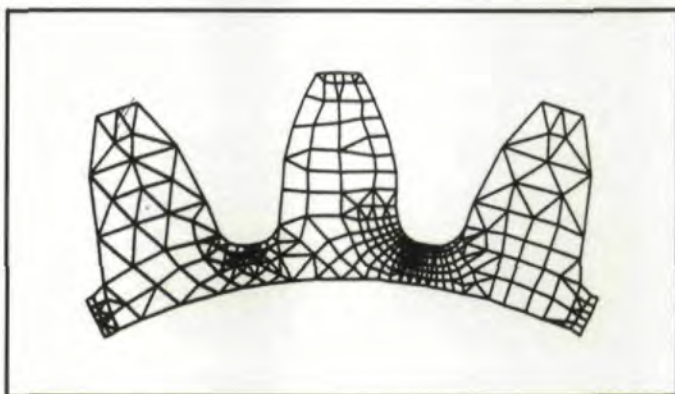


Fig. 10—Finite element model for case 4.

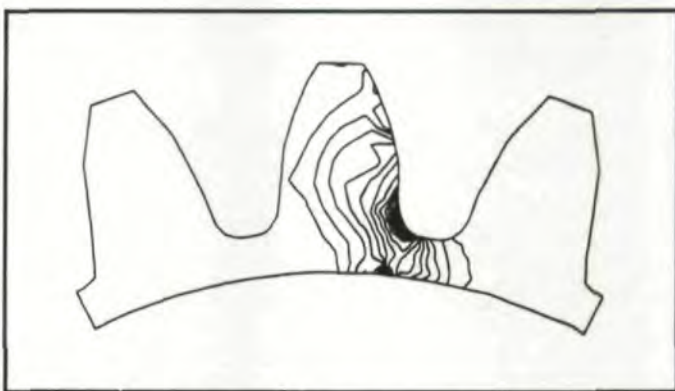


Fig. 11—Contour plot of maximum principal stress in the finite element model of case 4.

Table 3. Variation of the geometry factor with the rim thickness

Inner radius (inches)	Ratio of rim thickness to whole tooth depth	Geometry Factor J
0.50	1.5	0.334
0.70	0.67	0.334
0.75	0.46	0.291
0.80	0.25	0.159

for a complete study, this method cannot replace full fledged three-dimensional finite element analysis, but only supplement it. The boundary element method does not allow stress computations on the boundary, but this limitation can be overcome by computing the stresses at two points near the boundary and extrapolating the values to the boundary. The time required to compute the system matrices varies as the square of the number of nodes. Thus, the efficiency of the method decreases as models get large. Also, unlike the finite element method, the matrices are not banded or symmetric. However, meshes with 100 to 120 nodes serve well enough, and these limitations do not cause any serious problems.

Since only preliminary results are presented here, a considerable amount of case history experience is needed in order to assess the potential of this method more accurately. In par-

ticular, there should be some corroboration between J factors computed by the boundary element method and those computed by the AGMA method. The following studies are anticipated in the next year to provide further verification of this method for the evaluation of geometry factors:

- Comparison of boundary element results with current AGMA analysis and with finite element analysis for a broad spectrum of gear and hob geometries. Computation time comparisons with finite element methods will also be made.
- Comparison of boundary element results with computational and experimental results in the literature for thin rimmed gears and internal gears.
- Determine the feasibility of using personal computers for

the geometry factor calculation using boundary elements.

- Enhance the program to take care of the roller boundary conditions and to allow models to incorporate a number of teeth greater than three.

Appendix

Boundary Element Method Equations

Boundary element methods use approximating functions that satisfy the governing elasticity equations within the outer periphery of the body being analyzed, but not the boundary conditions. These functions are called the fundamental solutions.

Figs. 12 & 13 show a typical body which is to be analyzed. The elasticity equations which govern the analysis have been presented here in tensor notation for the sake of conciseness.

For every point in the body of interest to be in a state of equilibrium, the stress field must satisfy the following equilibrium equation:

$$\text{equilibrium: } \sigma_{ij,j} = 0 \text{ in } \Omega$$

Here i and j vary from 1 to 2 for a two-dimensional analysis and Ω is the interior of the body.

The surface loads or the tractions applied to the body are related to the stresses as

$$\text{traction: } \sigma_{ij}n_j = p_i \text{ (prescribed on } \Gamma_2)$$

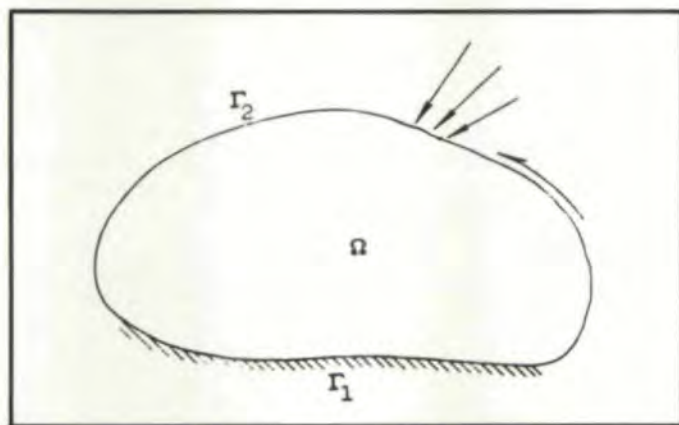


Fig. 12—Body under consideration.

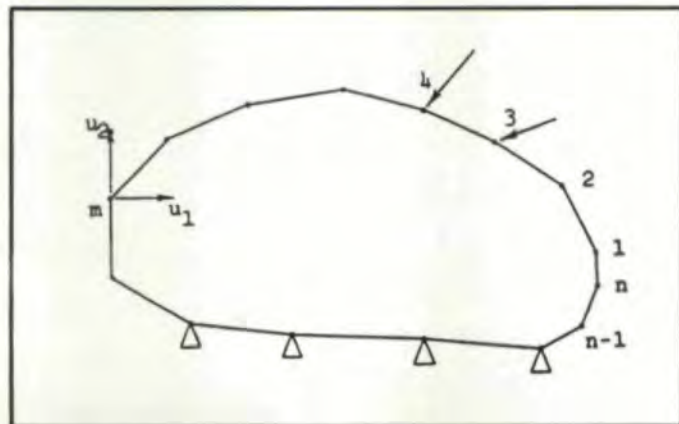


Fig. 13—Boundary element discretization.

These tractions are prescribed on part of the body's surface Γ_2 . On the rest of the surface of the body, the displacements u_i have to be prescribed. σ_{ij} is the stress tensor field and the u_i is the displacement vector field. The starting point for both the boundary element method and the finite element method is an integrated form of the equilibrium equation:

$$\text{for all } u_i^*: \int_{\Omega} u_i^* \sigma_{ij,j} d\Omega = 0$$

where u_i^* is an arbitrary weighting function. The choice of this weighting function is one of the differences between the boundary and finite element method. In the finite element method, these functions are chosen to be the same as the shape functions, whereas, in the boundary element method, the fundamental solutions are used.

Integrating by parts, (integration by parts in two and three dimensions is carried out using Green's identity) we get:

$$\int_{\Gamma} u_i^* \sigma_{ij} n_j d\Gamma - \int_{\Omega} u_{i,j} \sigma_{ij} d\Omega = 0$$

But it can be shown that

$$u_{i,j} \sigma_{ij} = \sigma_{ij} \epsilon_{ij}$$

Therefore, the integral becomes:

$$\int_{\Gamma} u_i^* \sigma_{ij} n_j d\Gamma - \int_{\Omega} \sigma_{ij} \epsilon_{ij} d\Omega = 0$$

or,

$$\int_{\Gamma} u_i^* p_i d\Gamma - \int_{\Omega} \sigma_{ij} \epsilon_{ij} d\Omega = 0$$

The above set of equations is characteristic of most finite element developments. However, the boundary element method carries out integration by parts once more:

$$\int_{\Gamma} u_i^* \sigma_{ij} n_j d\Gamma - \int_{\Omega} \sigma_{ij} \epsilon_{ij} d\Omega = 0$$

As before,

$$\int_{\Gamma} u_i^* \sigma_{ij} n_j d\Gamma - \int_{\Omega} \sigma_{ij} u_{i,j} d\Omega = 0$$

and using Green's identity to integrate by parts once more, for all u_i^* ,

$$\int_{\Gamma} u_i^* \sigma_{ij} n_j d\Gamma - \int_{\Gamma} u_i \sigma_{ij}^* n_j d\Gamma + \int_{\Omega} u_i \sigma_{ij,j} d\Omega = 0$$

If we choose the field u_i^* to be the response to a unit concentrated load at point P in the k direction, (Such a field is called a fundamental solution of the equilibrium equation.) then:

$$\sigma_{ij,j}^* + \delta_{ik} \Delta(P) = 0$$

Where δ_{ik} is the Kronecker delta and $\Delta(P)$ is the Dirac delta

function.

Hence,

$$\int_{\Omega} u_i \sigma_{ij}^* d\Omega = - \int_{\Omega} u_i \delta_{ik} \Delta(P) d\Omega = -c_p u_k(P) \quad (A.1)$$

where

$c_p = 0$ if P lies outside

$c_p = 1$ if P lies inside

$c_p = 0.5$ if P lies on a smooth boundary

In the general case, c_p has to be determined by integration.

We then have:

$$\int_{\Gamma} u_i^* \sigma_{ij} n_j d\Gamma - \int_{\Gamma} u_i \sigma_{ij}^* n_j d\Gamma - c_p u_k(P) = 0$$

but $\sigma_{ij} n_j =$ traction vector $= p_i$

$$\int_{\Gamma} u_i^* p_i d\Gamma - \int_{\Gamma} u_i p_i^* d\Gamma - c_p u_k(P) = 0$$

To make this equation discrete, let $u_i = \psi_m u_{mi}$ and $p_i = \psi_m p_{mi}$, where ψ_m are the shape functions defined along the boundary of the body only. We do not need to interpolate u_i and p_i inside the body because the above integral is to be evaluated only on the boundary.

The quantities u_{mi} and p_{mi} are the nodal values of the displacements and the tractions, respectively. At any given node, either u_{mi} or p_{mi} is known and the other value is unknown.

For every source point P and every direction k, we can make the above integral equation discrete to get one linear equation relating the p_{mi} and the u_{mi} . A new point P is then moved from one nodal point to the next and as many equations are generated as there are unknowns. This gives a system of linear equations:

$$[\bar{H} - C] u = [G] p$$

i.e.

$$[\bar{H} + C] u = [G] p$$

The matrix [C] contains all of the c_p coefficients. Instead of evaluating them by integrating, an easier way to determine them is by applying rigid body displacements and zero tractions in the above matrix equation.

The system of equations becomes:

$$[H] u = [G] p$$

which is then solved to determine the unknown tractions and displacements.

Once all of the nodal displacements and tractions are known, Equation (A.1) can be used to determine the displacement of any interior point P. This displacement can then be differentiated to obtain the strains and hence the stresses in the interior of the body.

References

1. AMERICAN GEAR MANUFACTURERS ASSOCIATION. *AGMA Standard For Rating the Pitting Resistance and Bend-*

ing Strength of Spur and Helical Involute Gear Teeth. AGMA 218.01, 1982.

2. S. K. WADHWA. "Analytical Determination of Geometry Factor for Shaped Spur Gears." ASME Paper 68-MECH-53, 1968.
3. R. G. MITCHNER. "The Determination of the Lewis Form Factor and the AGMA Geometry Factor J for External Spur Gear Teeth." ASME Paper 80-DET-59, 1980.
4. R. ERRICHELLO. "An Efficient Algorithm for Obtaining the Gear Strength Geometry Factor on a Programmable Calculator." AGMA Paper P139.03, 1981.
5. R. ERRICHELLO. "An Efficient Algorithm for Obtaining the Gear Strength Geometry Factor for Shaper Cut Gears." AGMA Paper P139.05, 1983.
6. R. J. DAVEY, R. T. WHEWAY. "An Exact Mathematical Solution for the Dimensions of the Lewis Equal Strength Parabola." ASME Paper No. 84-DET-183, 1984.
7. RAYMOND J. DRAGO. "Limitations of Current Tooth Root Stress Analysis." AGMA Paper No. 220.20, 1976.
8. RAYMOND J. DRAGO, GARY A. PIZZIGATI. "Some Progress in the Accurate Evaluation of Tooth Root and Fillet Stresses in Lightweight, Thin-Rimmed Gears." AGMA Paper 229.21, 1980.
9. TOSHIYUKI SUZUKI, TAE-HYONG CHONG, TOSHIO AIDA, HIROSHIGE FUJIO, AIZOH KUBO. "Tooth Fillet Stresses of Gear with Thin Rim." *Bulletin of the JSME* Vol. 25, No. 204, June, 1982, 1022-1029.
10. TAE-HYONG CHONG, A. KUBO. "Simple Stress Formulae for a Thin Rimmed Spur Gear. Part 1: Derivation of Approximation Formulae for Tooth Fillet and Root Stresses." ASME Paper No. 84-DET-62, 1984.
11. JÄRMO ELORANTA, ERIK SANDBERG. "Stress, Deflection and Load Distribution in Thin Rimmed Internal Gears." Second World Gear Congress, Paris, France, March 3-5, 1986. Manufacturing and Checking, 1986.
12. G. CASTELLANI, V. P. CASTELLI. "Rating Gear Teeth." ASME Paper No. 80-C2/DET-88, 1980.
13. TAE-HYONG CHONG, TOSHIYUKI SUZUKI, TOSHIO AIDA, HIROSHIGE FUJIO, AIZOH KUBO. "Tooth Fillet Stresses of Gear with Thin Rim." *Bulletin of the JSME*. Vol. 26, No. 214, April, 1983, 633-640.
14. TAE-HYONG CHONG, TOSHIYUKI SUZUKI, AIZOH KUBO, HIROSHIGE FUJIO. "Tooth Fillet Stresses of Gear with Thin Rim." *Bulletin of the JSME*. Vol. 26, No. 220, October, 1983, 1799-1806.
15. TAKESHI ISHIDA, TERUAKI HIDAKA, HIDEHARU TAKIZAWA. "Bending Stress Analysis of the Idle Gear with Thin Rim." *Bulletin of the JSME*. Vol. 28, No. 241, October, 1985, 2422-2428.
16. TAKESHI ISHIDA, TERUAKI HIDAKA, HIDEHARU TAKIZAWA. "Bending Stress Analysis of Idle Gear with Thin Rim." *Bulletin of the JSME*. Vol. 28, No. 244, July, 1985, 1505-1511.
17. RAYMOND J. DRAGO, RONALD V. LUTTHANS. "An Experimental Investigation of the Combined Effects of Rim Thickness and Pitch Diameter on Spur Gear Tooth Root and Fillet Stresses." AGMA Paper P229.22, 1981.
18. TAE-HYONG CHONG, A. KUBO. "Simple Stress Formulae for a Thin Rimmed Spur Gear. Part 2: Tooth Fillet and Root Stress Calculation of a Thin Rimmed Internal Spur Gear." ASME Paper No. 84-DET-63, 1984.
19. TAE-HYONG CHONG, A. KUBO. "Simple Stress Formulae for a Thin Rimmed Spur Gear. Part 3: Examination of the Calculation Method and Stress State of Internal Spur Gear." ASME Paper No. 84-DET-64, 1984.
20. TAE-HYONG CHONG, NAOTO KATAYAMA, AIZOH KUBO, HIROSHI YABE. "Tooth Fillet Stresses of Gear with Thin Rim." *Bulletin of the JSME*. Vol. 27, No. 224, February, 1984, 325-332.
21. TAE-HYONG CHONG, NAOTO KATAYAMA, AIZOH KUBO, HIROSHI YABE. "Tooth Fillet Stresses of Gear with

the geometry factor is directly determined so that it may be used in the current AGMA 218.01 rating standard. Since the AGMA method currently in use is a two-dimensional analysis method, the authors decided to use a two-dimensional boundary element. Note, however, that in many complex root stress problems, three-dimensional analyses should be used in order to obtain accurate stress results. Gakwaya et al⁽²⁷⁾ show comparisons of the computational time required by the boundary element method and the finite element method. Holze⁽²⁹⁾ discusses advantages and disadvantages of the boundary integral equation method and compares it with the finite element method for a plane-stress gear-tooth problem.

Boundary Element and Finite Element Methods

The finite element method divides the body that is being studied into many pieces or elements whose behavior is easier to approximate than that of the whole body. The equations describing each element are "assembled" in a system of linear equations and are then solved.

The boundary element method, on the other hand, does not divide the body under consideration into elements. For a homogenous, isotropic body with no body forces, the only causes for displacements and stresses within the body are loads and displacements applied along the boundary. The body can be considered to be part of an infinitely extending material which is subjected to loads along the original boundary. Thus, if a function which describes the response of an infinitely extending medium to a point load is known, then this function can be used to compute the response of the body by moving the point load along the boundary and integrating each individual response. Therefore, the integration which is carried out numerically by breaking the boundary into elements only needs to be carried out along the boundary. The boundary element method has the advantage of not requiring that the interior of the body be divided into two-dimensional elements with only the boundary being divided into one-dimensional elements. Because of its mathematical complexity and because other references, such as Brebbia,⁽²⁵⁾ provide the mathematical details of the boundary element method, its theoretical basis is not presented in this article. However, a summary of its theory is presented in the Appendix.

An important advantage of the boundary element method is that it is usually able to represent areas of stress concentration and singularities better than general purpose finite element methods. Because only the boundary needs to be made discrete in boundary element methods, it is possible to work with smaller systems of equations and arrive at very accurate results.

Boundary Element Mesh Generator and Boundary Element Program

The problem of writing a finite element mesh generator which is capable of creating good meshes for all possible types of gear teeth and for many types of shapes is complicated; whereas, writing a boundary element mesh generator is a somewhat simpler task. It is possible to devise a mesh generation scheme that in two dimensions works very well for all kinds of gear teeth with an assortment of shapes.

In the boundary element mesh generator used in the follow-

ing numerical examples, the only input data required is a description of the hob that is used to cut the gears (or the gear shaper, in the case of the internal gears).

The generator program computes the position and unit normal vectors at a number of points on the hob and uses these values to compute the positions of the corresponding points on the gear by using the conjugacy equations. Fig. 1 shows the hob generating the geometry of a side of a gear tooth. Undercutting is detected numerically. The boundary of the gear tooth is divided into several segments, and the user is asked to input the number of boundary elements into which each segment is to be divided, as shown in Fig. 2.

The meshes generated by this program model three teeth,

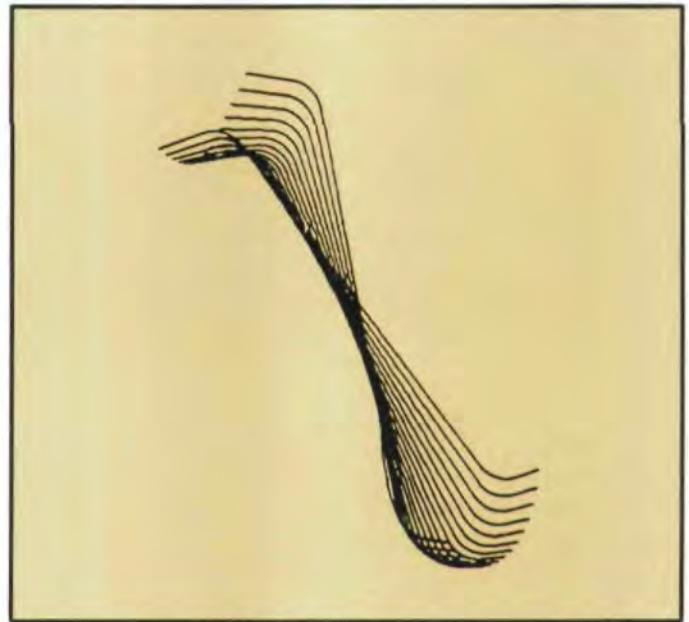


Fig. 1—The process of generating the gear tooth geometry from the hob geometry.

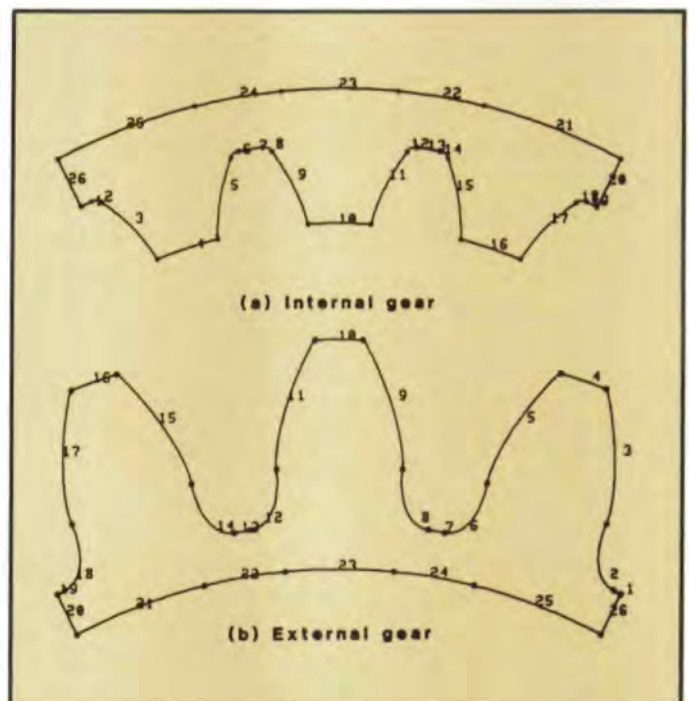


Fig. 2—Gear tooth boundary and its subdivision into segments.

Table 1. Results of test cases

Mesh	Number of teeth	Radius of inner bore (outer radius for int. gear)	Ratio of rim thickness to whole tooth depth	Radius at point of max. stress from BEM	J Factor by the BEM	J Factor by the FEM
1	20	0.7"	0.67	0.864"	0.335	0.310
2	20	0.7"	0.67	0.864"	0.343	0.319
3	20	0.8"	0.25	0.856"	0.159	0.135
4	20	0.8"	0.25	0.876"	0.389	0.356
5	20	0.95", 1.2"	0.67	1.100"	0.123	—
6	20	0.95", 1.2"	0.67	1.100"	0.412	—
7	12	0.3"	0.67	0.478"	0.255	—

with the load being applied on the center tooth. Three teeth are used to accurately model the effects of rim thickness and of boundary conditions on the root stresses. The current program provides two means of constraining the model, the first being to fix all sides of the tooth support, and the other being to fix only the ends of the rim and to leave the inner bore free. Other possible ways of constraining the teeth that are to be implemented in the future include roller and contact type boundary conditions. The mesh that is generated can be modified to account for features such as keyways and weight reducing holes. It was found advisable not to make the mesh too coarse at the point of load application or at the supports.

The user is given a choice of either specifying the radius at which a unit normal load is applied on the involute part of the profile, or letting the program compute the highest point of single tooth contact and applying the load there. The user is also given the choice between plane strain and plane stress conditions for the gear tooth model. The choice between these two conditions depends on how wide the gear tooth is in relation to its other dimensions.⁽³⁰⁾

The meshes generated by the above mentioned mesh generator are sent to a general two-dimensional boundary element program written by the authors. The boundary element method does not allow computation of stresses on the boundary because of the numerical behavior of the fundamental solution, which imposes a restriction similar to the finite element method, where one computes stresses only at

Gauss points. This program computes the displacements of the nodes of the mesh and then searches along the boundary for the maximum stress at the boundary. Stresses at the boundary are calculated by computing stresses at both one element length and one-half element length from the boundary and then extrapolating stresses to the boundary. The multi-axial state of stress at all points is converted into an effective stress using one of the many available multi-axial theories of failure. In the numerical examples that follow, the maximum principal stress is used as the failure criterion.

As per the defining equation of the J factor in the AGMA standard 218.01,⁽¹⁾

$$s_t = \frac{(K_a K_s K_m)}{K_v} \left(\frac{W_t P_d}{F J} \right)$$

where

- K_a is the application factor,
- K_s is the size factor,
- K_m is the load distribution factor,
- K_v is the dynamic factor,
- F is the face width,
- W_t is the transmitted load,
- P_d is the diametral pitch and
- J is the geometry factor.

The stress s_{BEM} that the boundary element method computes includes the effect of the geometry that the J factor represents, but does not include the effects of the application, size, load distribution and dynamic factors. Therefore,

$$s_{BEM} = \left(\frac{W_t P_d}{F J} \right)$$

so that the J factor can be computed from the stress value s_{BEM} .

Numerical Examples

Table 1 describes the seven gears used for the numerical examples, and Table 2 gives the geometry of the hob that was used for all the external gears. Mesh 1 (Fig. 3) is a thick rimmed gear, whose rim is not constrained, and Mesh 2 (Fig. 4) is the same gear, whose rim is constrained. The location

(continued on page 33)

Table 2. Dimensions of the Hob used to Cut the External Gears used in the Test Cases.

Diametral pitch	10.0
Pressure angle of the rack	20°
Addendum constant of hob	1.4
Dedendum constant of hob	1.0
Corner radius at tip of the hob tooth	0.02 in
Fillet radius at root of the hob tooth	0.02 in